[논 문] 한국재료학회지
Korean Journal of Materials Research
Vol. 3, No. 5 (1993)

Characterization of Surface Damage and Contamination of Si Using Cylindrial Magnetron Reactive Ion Etching

Geun-Young Yeom

Department of Materials Engineering, Sung Kyun Kwan University

Abstract Radiation damage and contamination of silicons etched in the CF_4+H_2 and CHF_3 magnetron discharges have been characterized using Schottky diode characteristics, TEM, AES, and SIMS as a function of applied magnetic field strength. It turned out that, as the magnetic field strength increased, the radiation damage measured by cross-sectional TEM and by leakage current of Schottky diodes decreased close to that of wet etched samples especially for CF_4 plasma etched samples. For CF_4+H_2 and CHF_3 etched samples, hydrogen from the plasmas introduced extended defects to the silicon and this caused increased leakage current to the samples etched under high magnetic field, even though it improved electrical properties of the samples etched at low magnetic field strength conditions by hydrogen passivation. The thickness of polymer residue on the etched silicon measured by TEM and the Auger depth profiling was also decreased with the increasing magnetic field strength and showed the minimum polymer residue thickness near the 100Gauss where the silicon etch rate was maximum. Also, other contaminants such as target material were found to be minimum on the etched silicon surface near the highest etch rate condition.

1. Introduction

In VLSI circuit fabrication, reactive ion-assisted etching (RIE) techniques are replacing wet etching and plasma etching techniques. In particular, these new techniques are rapidly becoming an essential requirement in the delineation of patterns less than 1㎛ due to their ability to provide anisotropic etch profiles. One application of interest is obtaining precise channel lengths and widths in MOSFET devices. Unfortunately, specimens processed by RIE are subject to radiation damage such as ion implantation, near surface modification, and residue formation on etched Si surfaces.

Etching by RIE or reactive ion beam etching has been studied by many researchers who have reported on the contamination[1~11] and radiation damage[12~26] induced by energetic ion bombardment to the samples. It has been shown by Fonash et al.[18] that reactive ion etching and ion beam etching using a variety of gases result in a damaged layer on the surface of etched silicons. Also, it has been shown that the damaged layer contains positive charges which can affect the electrical characteristics of the samples. Pang et al.[13] have shown that MOS capacitors fabricated on the Si surfaces processed with dry etching display increased interface state densities which are strongly dependent on the ion species and energy. Samples etched with CHF_3+O_2 plasmas have been examined using Transmission electron microscopy(TEM) by Cerva et al.[21] to investigate the depth of damaged layer. They found a polymer layer of a few tens of nanometers in thickness and a damaged layer of several hundreds nanometers deep on the etched silicon surface. Contamination or surface residues caused by reactive ion etching in CF_4+H_2 gas mixtures have been studied by Oehrlein et al.[3,5,6,10] using X-ray photoelectron spectroscopy(XPS). They showed that the change of residue thickness is responsible for

Si etch rate. As a result, a diffusion-limited Si etch mechanism has been suggested.

Ion bombardment damage of Si resulting from planar magnetron reactive ion etching has been studied by Hirobe et al.[27] in a high pressure range (a few hundreds mTorr) using CHF_3+SF_6 gas mixtures. By using Reflected high energy electron diffraction (RHEED) and by measuring minority carrier lifetime, they showed that radiation damage decreased with increasing applied magnetic field strength. The residue of magnetron etched samples at about 200Gauss of magnetic field was compared with reactive ion etched samples by Oehrlein et al[28] in 1988. They observed that the thickness of residue layer of the magnetron etched samples was less than that of reactive ion etched samples.

In this paper, experimental results are reported on which the effect of magnetic field strength on the degree of radiation damage and contamination of Si samples etched in cylindrical magnetron dicharges. The samples were etched at a fixed power density and with different gas mixtures. Even though previous studies by other researchers showed that magnetron reactive ion etching may reduce radiation damage and contamanation, more experiments were needed to quantify the effects of magnetic field strength on the radiation damage and the degree of contamination in a pressure range of a few mTorr which gives highly anisotropic etch profiles of interest.

II. Experimental Procedures

The equiment and silicon etch conditions for the experiment are described elsewhere[29~31]. In general, silicon samples were etched in 3mTorr CHF_3 or CF_4/H_2 gas mixtures and at a fixed power density of $0.45-0.75W/cm^2$. The magnetic field strengths applied to the plasmas were varied from 0 to 250Gauss. All of the samples were exposed to the plasma until 1.5 ㎛ of Si was etched away.

A. Characterization of Radiation Damage

To study the degree of radiation damage, cross-sectional transmission electron microscopy(TEM) and I-V characteristics of Schottky diode fabricated from the etched silicons were used. The first method was used to study the degree of physical damage and the second was used to study the degree of electrical damage of etched samples.

Blank Si wafers with no photolithographic pattern on them were used to study the degree of radiation damage. Special precautions were followed before and after the etching of the samples. Before the etching, the samples were cleaned with H_2SO_4 mixed with H_2O_2(H_2SO_4 : H_2O_2 4 : 1) at 90℃ for 20 minutes for degreasing, and dipped in a 10% HF solution for 5 seconds to remove any native SiO_2. For the I-V characteristics, sample were cleaned again using the method described above after the etch.

Transmission electron microscopy(Philips EM400, acceleration voltage : 120kV and Philips EM430, acceleration voltage : 300kV) was used to study the thickness of residue layer formed on Si surface during the etching. Some of the samples were overcoated with 200Å of Al to help to identify the residue layer. All of the samples prepared at various conditions, regardless of Al deposition, were cleaved along <110> direction into two pieces. The etched surfaces were glued together with M-Bond 610 Adhesive. The glued samples were compressed together and heated at 150℃ for 150 minutes to increase the sticking of the glue to the samples. These samples were cut into pieces along the direction perpendicular to the cleaved direction. The samples were thinned down to a direction parallel to the etched surfaces(etched surfaces are now facing each other) using mechanical polishing and ion milling to examine the cross section of the sample interface with TEM. TEM micrographs were taken along the <110> zone axis to see the etched surface vertical to the viewing plane. The defects (dislocations and point defects)

were observed using TEM to indicate radiation damage. However, the number of detected defects increased as the sample thickness in the viewing area increased. To compare the degree of damage at various conditions, the same sample thickness at the sampling area was needed. The sample thickness was approximately examined by tilting the specimen about 30 degrees and measuring the increase of the thickness of deposited aluminum. Fortunately, for our experimental conditions, the variation of defect densities were not sensitive to the sample thickness compared to that by the variation of magnetic field strength.

To make Schottky diodes, the etched samples were cleaned by the method described above, and 2000Å thick Au was deposited using a resistively heated evaporator and were patterened using a lift-off process. The photomask for Schottky contacts had 0.2mm diameter open dots on it. On the back side of the samples, 2000Å thick aluminum was blank deposited using an electron beam evaporator to make an Ohmic contact. The I-V characteristics were measured using a semiconductor parameter analyzer(HP 4145A) in a light tight probe station. As an estimation of radiation damage, reverse saturation current were measured and compared to those of reference samples which were wet etched in 10% HF solution.

B. Characterization of Surface Contamination

To study the degree of contamination on the etched samples, Auger electron spectroscopy (AES) and secondary ion mass spectroscopy (SIMS) were used. AES(Perkin Elmer, PHI 25-120) surface survey was used to study the composition and species of residue layer and AES depth profile was used to estimate the thickness of residue layer. SIMS(CAMECA IN35f) depth profiling was used to look for the contamination species that can not be detected using AES such as hydrogen. Most of the contamination species detected by the SIMS depth profile were the species that penetrated into silicon by ion bombardment. Therefore, it was also related to radiation damage. All of the sample were exposed to the plasma until 1.5μm of Si was etched. The samples were cleaned before etching by the methods described above and were kept intact after the etching.

Ⅲ. Experimental Results

A. Characterization of Radiation Damage

It has been known that three layers on the surface may be present when Si is exposed to RIE[2,18,32]. These layers are not sharply defined ; rather they gradually blend into one another. The schematics of these three layers are shown in Fig. 1. The uppermost layer is C-F polymer residue which was formed during the reactive ion etching and will be discussed in the next section. The second layer is a heavily damaged crystal where the Si surface is severely deformed. This layer is formed primarily by the implantation of positive ions from the plasma driven by dc self-bias voltages developed on the powered electrode[2,32]. This layer is a few nanometers in thickness[2,4,22] The third layer is lightly damaged and appears to be a result of diffusion of active species. The diffusion may form dislocations, vacancies, and interstitials, extending several tens of nano-

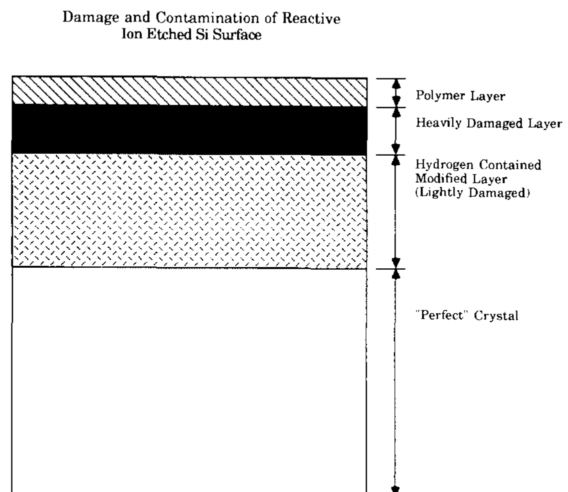

Fig. 1. Schematic diagram of radiation damage below and contamination on the etched silicon surfaces.

nanometers. The two lower layers affect the electrical properties of etched Si.

The change of electrical properties resulting from radiation damage by cylindrical magnetron discharges has been investigated by measuring I-V characteristics of Schottky diodes and physical properties have been studied using cross-sectional TEM. The I-V characteristics of Schottky diodes were obtained from the previous experimental results[31].

a. Reverse Saturation Current of Schottky Diodes

It has been shown by Fonash et al.[7,14,15,17,25] that the I-V characteristics of Schottky diodes made after the exposure to reactive ion etching or ion beam etching are very sensitive to the degree of radiation damage. Also, they have verified that the exposure to the plasma introduces positive charges into Si which changes the effective barrier height of the Schottky diode.

Reverse saturation currents of Schottky diodes made from magnetron etched samples which were published previously[31] are shown in Fig. 2. The reverse saturation currents of the Schottky diodes were extracted from the I-V characteristics of the diodes. The samples were processed in 3mTorr CF_4+H_2 and

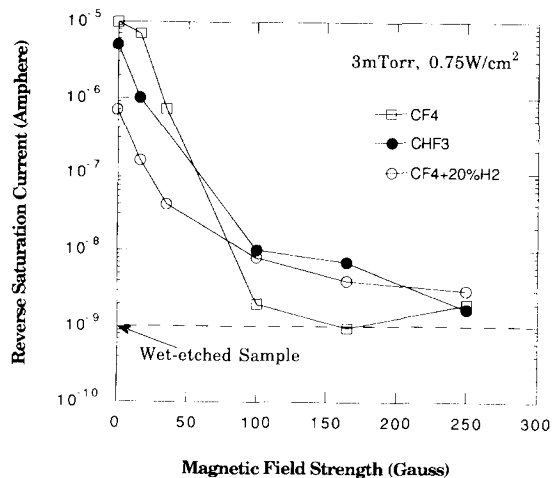

Fig 2. The reverse saturation current (leakage current) of Schottky diodes made from etched Si for various gas mixtures at different magnetic field conditions. The dotted line is the leakage current for a wet-etched sample.

CHF_3 plasmas at a power density of $0.75W/cm^2$. The reverse saturation currents of the samples exposed to the magnetron plasmas was compared with that of a wet-etched sample which was not exposed to the plasma. The magnetic field strength to the plasmas was varied from 0 Gauss to 250Gauss. As shown in the figure, as the magnetic field strength increased, the reverse saturation currents of Schottky diodes previously exposed to the plasma decreased from $10^{-5}-10^{-6}$ A to near 10^{-9} A which was close to the leakage current of Schottky diode measured for wet-etched samples. These effects are responsible for the change in the effective barrier height[16,33]. In general, the reverse saturation current (J_s) is related to the effective barrier height (ϕ_n) of Schottky diode from the equation[34]:

$$J_s = A^* T^2 \exp(-q\phi_n/kT)$$

Where A^* is effective Richardson constant (110 for N-type Si) and T is absolute temperature. Fonash et al.[24] showed that the I-V curves of Schottky diodes made from RIE etched samples approach those of wet-etched samples as the annealing temperature is increased or as the damaged layer is removed. Consequently, the effective barrier height calculated from the saturation current increased to the ideal barrier height of Schottky diode. We therefore interpret our results as stating that as the magnetic field strength increases in a cylindrical magnetron discharges, Si samples receive less radiation damage.

It is seen from the figure that at low magnetic field strengths, the leakage currents of Schottky diodes previously exposed to $CF_4+20\%H_2$ plasmas. However, at the high magnetic field strength conditions, the leakage currents of Schottky diodes previously exposed to CF_4 plasma are smaller than those of the other conditions.

For reactive ion etched samples, Fonash et al.[14,15] have shown that the addition of hydrogen to CF_4 plasma causes the saturation of dangling bonds on the etched surface which results from the ion bombardment. Therefore, the addition of hydrogen reduces extra states in the band

gap of Si and helps to recover the I-V characteristics of damaged Schottky diodes close to the ideal I-V characteristics. In our samples with low magnetic field strength, the low leakage current for the diodes etched with CF_4+20%H_2 or CHF_3 plasmas appears to result from this effect. For CHF_3 plasmas, hydrogen atoms are available from the dissociation of CHF_3 and have been observed from optical emission spectroscopy. At high magnetic field strengths where the ion energies impinging the surface are small, hydrogen appears to have an effect different from the saturation of dangling bonds in Si. It appears that excess hydrogen itself may introduce electrical defects. When the necessity for passivation by hydrogen atoms is

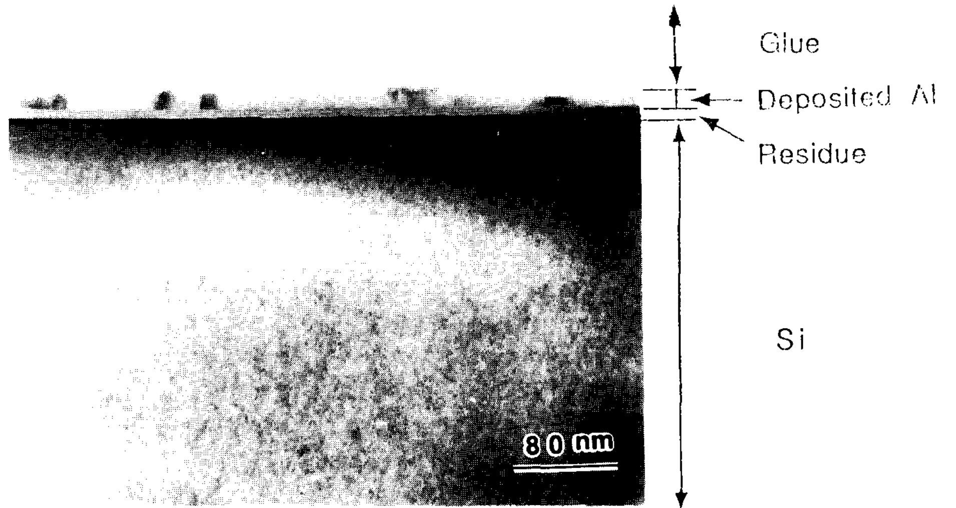

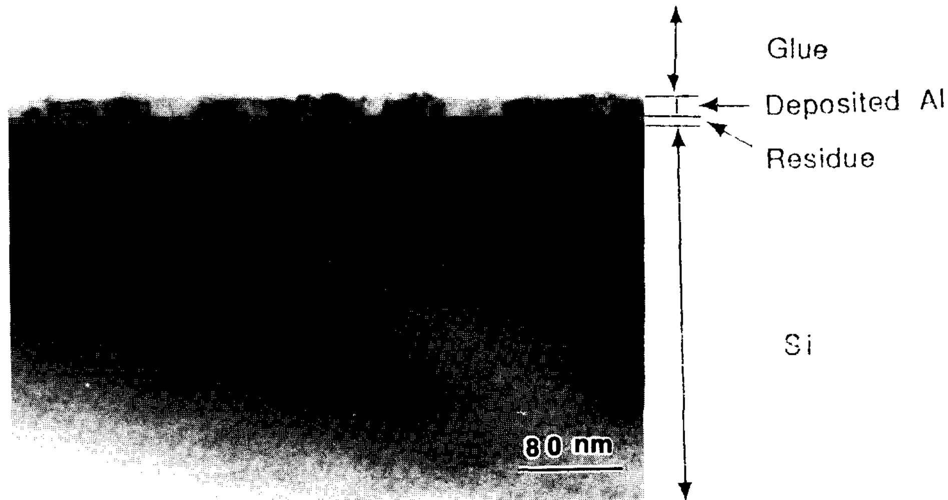

Fig 3. Transmission electron micrographs showing the(110) cross-section of Si surface etched 1.5㎛ in thickness at 0Gauss. To distinguish the residue layer from the glue layer, a 20nm thick aluminum layer was deposited on top of the Si. a) CF_4 plasma etched Si; b) CF_4+20%H_2 plasma etched Si.

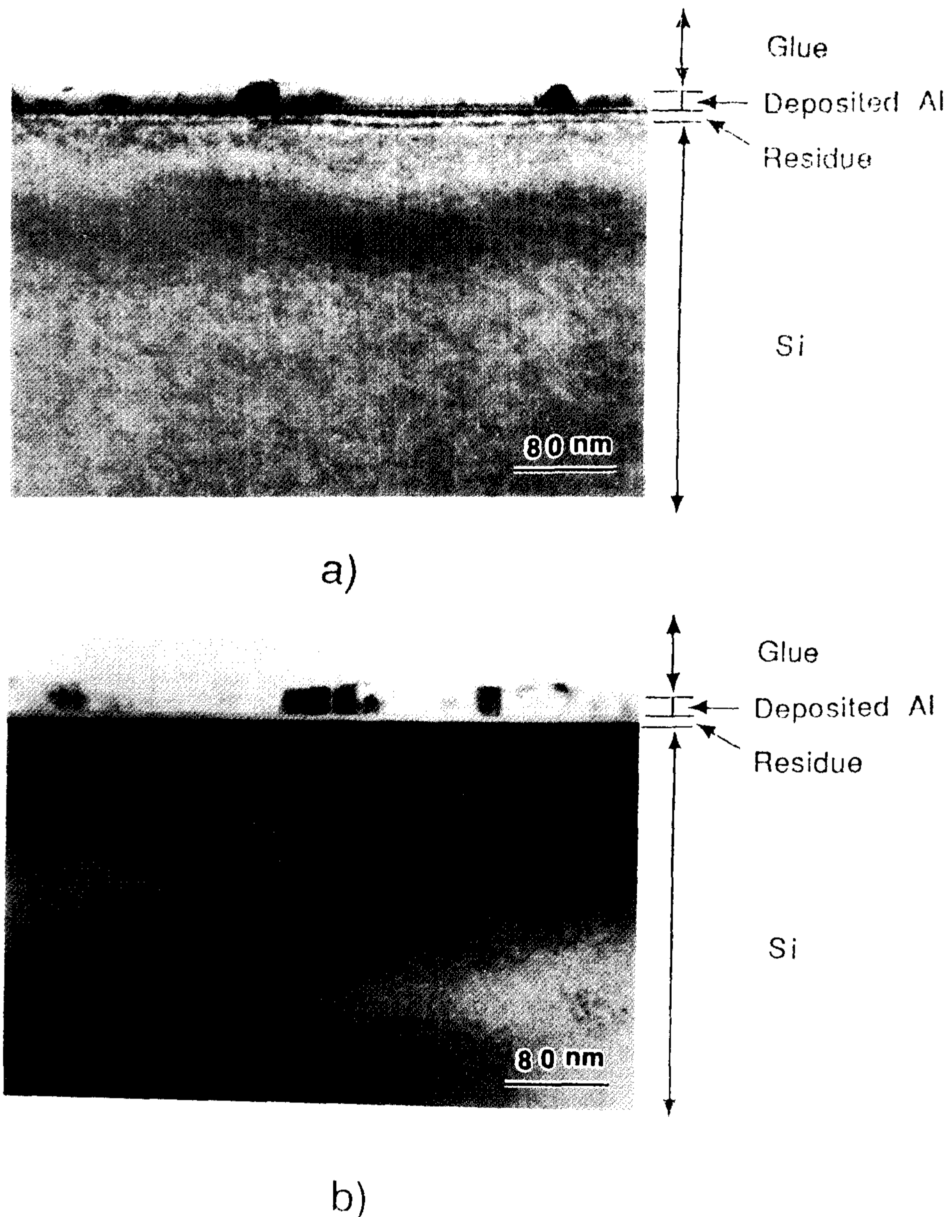

Fig. 4. Transmission electron micrographs showing the(110) cross-section of Si surface etched 1.5μm in thickness at 100Gauss. a) CF_4 plasma etched Si; b) CHF_3 plasma etched Si.

removed by reducing radiation damage, the detrimental effects remain.

b. Transmission Electron Microscopy(TEM)

The effect of added hydrogen in the discharge on radiation damage can be seen by comparing bright field images shown in Fig. 3 for a CF_4 plasma etched sample and a CF_4+20%H_2 plasma etched sample at 0Gauss. In Fig. 4 samples are compared for CF_4 plasma etching and CHF_3 etching at 100Gauss. The CF_4 treated sample, as shown in Fig. 3 (a), has a heavily damaged layer of less than 2nm. The damage appears as a dark line in the micrograph near the surface. The dark band shown in the picture is actually a thickness fringe not the damage. It appears that the damage is

present on the surface but other visible defects were not found in the Si surface deeper than 2.5nm. To distinguish the polymer layer deposited from plasma processing with a layer of glue used to prepare TEM specimen, a 20nm thick aluminum layer was deposited, shown as a polycrystalline structured layer in the figure. The polymer layer is seen between the aluminum deposited layer and the heavily damaged Si surface. The thickness of the polymer layer was about 5nm. For the sample treated with a $CF_4+20\%H_2$ plasma shown in Fig. 3 (b), the heavily damaged layer was about 55nm in thickness and no extended defects were found. The thickness of the polymer layer was about 6.5nm. For the samples etched at 100Gauss shown in Fig. 4, the polymer thickness of the CF_4 plasma etched sample was about 2.5nm and that of the CHF_3 plasma etched sample was about 5.5nm. The thickness of the heavily damaged layer has decreased to 10nm for the CHF_3 etched sample. However, this sample showed some visible defects having either short dislocation loops or point defects up to 150nm deep in thickness.

The differences in thickness of damaged layer between the samples etched with $CF_4+20\%H_2$ and CHF_3 plasmas and the that etched with CF_4 plasmas are caused by hydrogen implantation at the Si surface. These result from the ion energies being accelerated by dc potentials on the target electrode. The bias voltages for the above conditions were similar to each other. (At 0Gauss conditions, the self-bias voltage of target electrode with a CF_4 plasma was 1000 ; for a $CF_4+20\%H_2$ plasma, it was 1050 V.) Hydrogen ions in the plasma penetrate into Si deeper than other plasma ions(CF_3^+, CF_2^+, CF^+, and C^+), and make deeper defects near the silicon surface. In Table 1, the depth of hydrogen ions penetrated in the Si surface is shown as calculated using TRIM[35]. In case of CF_4/H_2 and CHF_3 plasmas, carbon also penetrates into Si. However, the concentration of carbon ions in the plasma is very small and the depth of penetration of carbon is much smaller than hydrogen ions. Therefore, the depth of damage should be smaller for a CF_4 plasma etched sampled than for a CF_4+H_2 or a CHF_3 plasma etched sample.

Table 1. Hydrogen penetration ans Si displacement ranges caused by ion implantation at various self-bias voltages associated with given magnetic field strengths. The energies of hydrogen ions were assumed to be same as the bias voltages.(Calculated by TRIM program)

Bias voltages and B field strength		Hydrogen		
		Ion Range		Max. Net
(V)	B field	Max(Å)	Min.(Å)	Displacement(Å)
60	100	90	29	0
300	32	210	87	96
800	16	440	181	280
1000	0	520	217	368

A comparison of the calculated value of mean ion range and measured thickness of the damaged layer in Fig. 3(b) and Fig. 4(b) showed that the measured layer is close to the calculated value. The dislocation loops and the point defects that are deeper than the hydrogen implantation thickness appear to be from hydrogen diffusion into Si.

More details of the effect of mangnetic field strength on the radiation damage of $CF_4+20\%H_2$ plasma etched samples are shown in Fig. 5. All of the samples were etched at a same power density of $0.75W/cm^2$ at 3mTorr pressure. For most of the samples, no aluminum layer was deposited on the samples before cross sectional TEM examination, therefore,

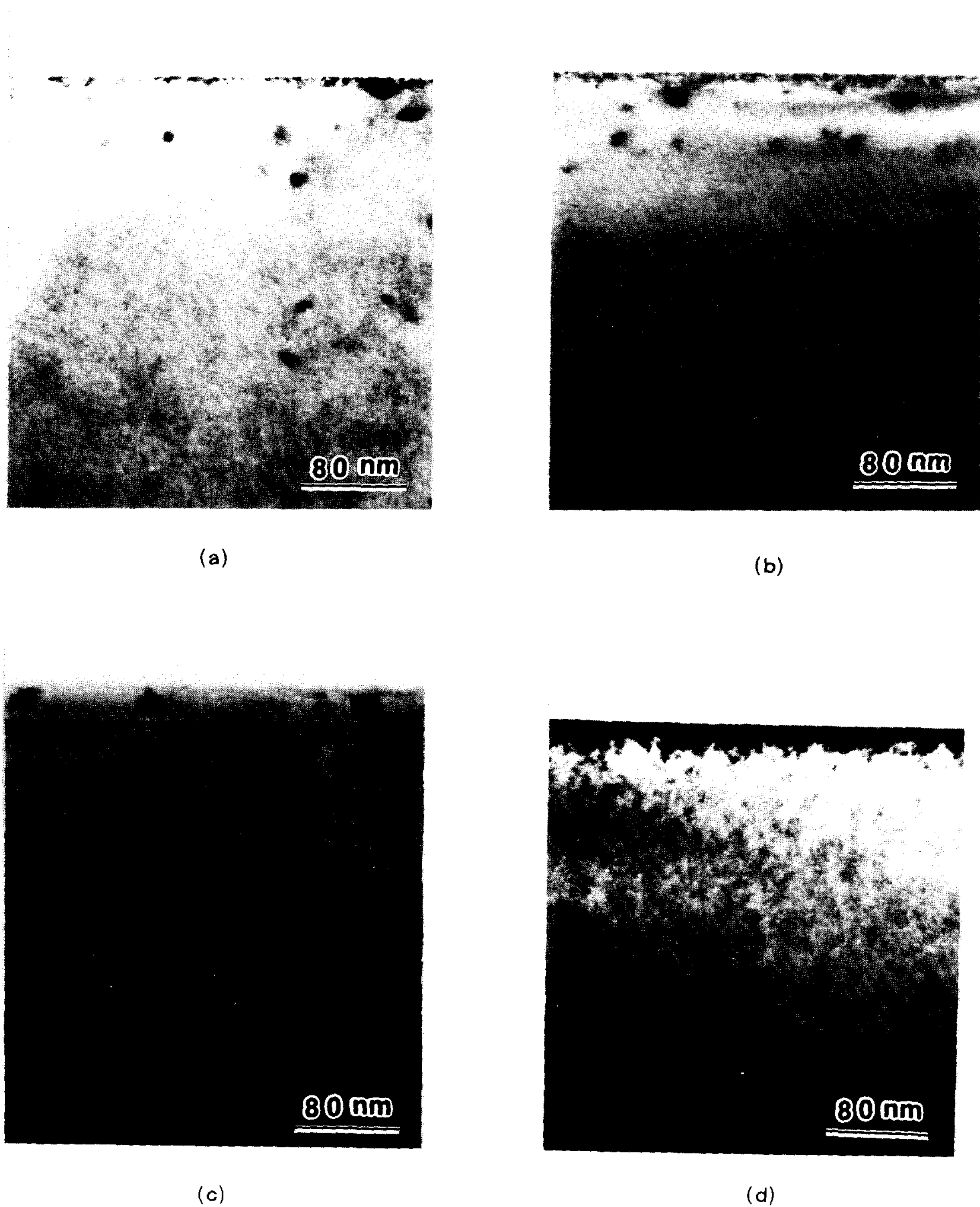

(a) (b) (c) (d)

Fig. 5. Transmission electron micrographs showing damage in the (110) cross-section of Si etched with CF_4 $+20\%H_2$ plasmas at various magnetic field. a) 250Gauss, b) 100Gauss, c) 16Gauss, d) 0Gauss.

polymer layer is not seen in those micrographs. In general, the depth of heavily damaged layer decreased with increasing magnetic field strength. This effect is attributable to the de-

crease of target bias voltage as the magnetic field strength increased, as demonstrated from TRIM calculations. However, the extended defects appear to be present at deeper positions for high magnetic field conditions as in Fig. 4 (b) when compared to the samples etched with 0Gauss. It appears that more diffusion into Si occurs at high magnetic field strengths possibly due to the sample heating during the processing at high magnetic field strengths. In Fig. 5, the extended defects were as deep as 225nm at 16 Gauss, and 375nm(deeper than the bottom of the picture) at 250Gauss, while being less than 50nm at 0Gauss.

Jeng et al.[22] studied hydrogen defects in Si in 1988 for D_2 plasma exposed samples and found many {111} planar defects distributed in the Si. A high resolution lattice image of our samples for the defects is shown in Fig. 6. Crossed lines in the figure are {111} atomic planes spaced at 3.12Å and the defects indicated by arrows are located {111} planes. Therefore the defects in our samples also appeared as {111} defects.

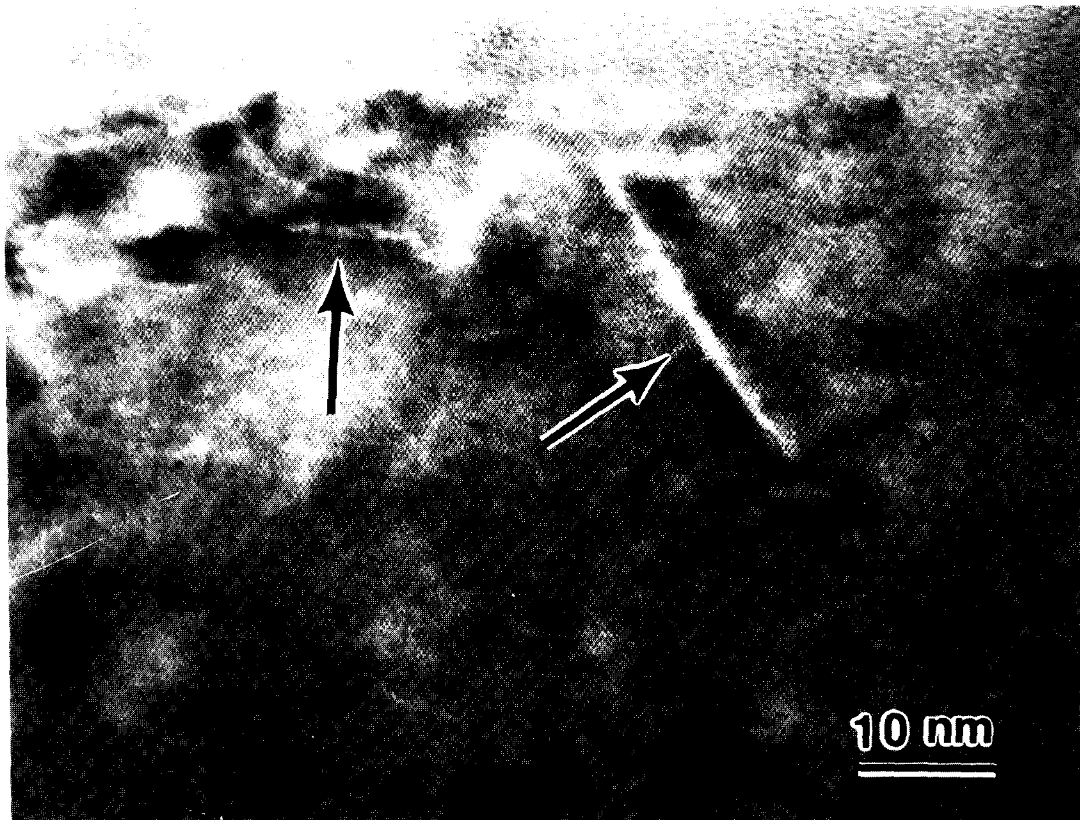

Fig. 6. A high resolution lattice image of etched Si surface showing {111} planar defects. The etch conditions was 0.75W/cm^2, 3mTorr CF_4 + 20%H_2, and 16Gauss. The sample was exposed to the plasma until 1.5 μm of silicon was etched.

B. Characterization of Surface Contamination

Reactive ion assisted etching with gas mixtures containing carbon results in a residue layer on Si surface. When CF_4+H_2 gas mixtures are used for reactive ion etching, it has been suggested that this residue layer plays an important role in the selectivity between Si and SiO_2[10]. That is, SiO_2 can be etched easily without forming a thick polymer layer because carbon forming the polymer layer can react with oxygen in SiO_2, thereby suppressing the formation of residue. However, Si etching is

suppressed when the polymer is formed on the surface because carbon arriving on the Si surface tends to form a residue instead of forming volatile species which leave the surface. The thickness of this polymer layer, its composition, and the chemical bonding state formed on the Si surface have been studied by many authors using AES[1,18,36], XPS[2~11], etc. These studies have shown that the thickness of polymer layer is as large as 3nm. Oehrlein and Williams[10] showed that for CF_4+H_2 plasmas using a Teflon electrode, the thickness of polymer increased as Si etch rate decreased when the residue thickness was larger than 1nm. Also, they suggested that Si etch mechanism is diffusion limited. The incoming F atoms diffuse towards the Si and outgoing SiF_4 diffuse through the residue layer towards the plasma. These combined effects control the Si etch rate.

The impurities implanted in Si and their chemical bonding states, along with the degree of lattice damage, were investigated using SIMS[9,37,38], RBS[2~6,17], Raman scattering[2], etc.

In our experiment, the composition and thickness of polymer layer on the etched Si was studied with AES. SIMS was also used to study other contamination species which can not be investigated with AES.

a. Auger Electron Spectroscopy(AES)

Surface analyses of the samples etched with CF_4 and $CF_4+35\%H_2$ plasmas as a function of magnetic field strength for a power density of $0.75W/cm^2$ at 3mTorr are shown in Fig. 7 and 8. C, O, F, and S were observed as major contaminants. The origins of carbon and fluorine are from the reactive gas used in the experiment. The oxygen appears to be from exposure to air before the surface analysis. However, the orgin of sulfur is not well understood. When the sensitivity factors of each component are considered, the fractional composition of each residue can be calculated. These values are shown in Table 2 for carbon, fluorine, and

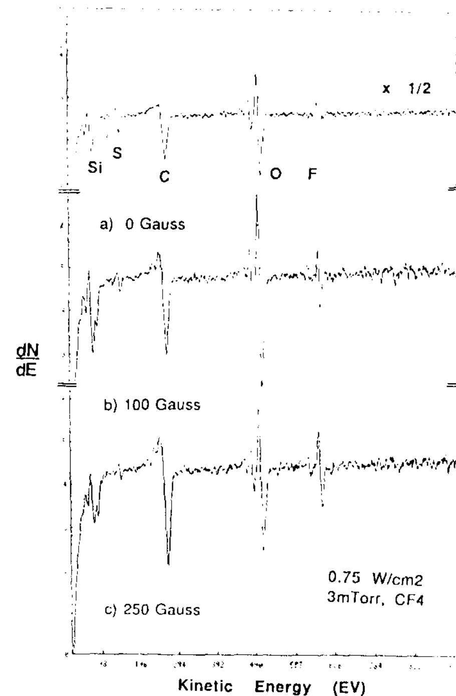

Fig. 7. Auger electron spectra of the Si surface etched with a CF_4 plasma at different magnetic field strengths. The total pressure was 3mTorr and the power density was $0.75W/cm^2$[2]

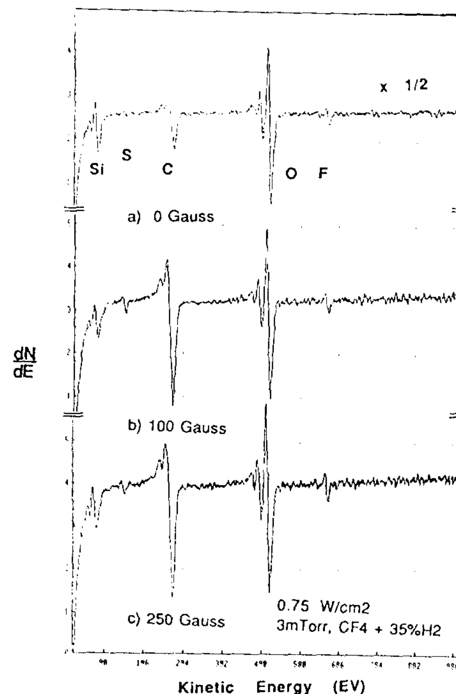

Fig. 8. Auger electron spectra of the Si surface etched with a $CF_4+35\%H_2$ plasma at different magnetic field strengths. The total pressure was 3mTorr and the power density was $0.75W/cm^2$[2]

oxygen.

The compositional change as a function of magnetic field strength in Table 2 shows that as the magnetic field strength increases up to 135Gauss, carbon atomic percent tends to increase while fluorine decreases. The C/F ratio of CF_4 plasma treated samples which was taken from Table 2 was less than that of CF_4+H_2 plasma treated samples. This may result from the fact that for CF_4+H_2 plasmas, hydrogen can react with fluorine by forming HF, and reduce F radical concentration in the plasma.

Table 2. Effect of magnetic field strength on the composition of the residue for Si samples exposed to CF_4 and CF_4+H_2 plasmas.(Power density : 0.75W/cm^2 Pressure : 3mTorr, H_2 is 35% for CF_4+H_2)

B Field Strength (Gauss)	Carbon(%)		Fluorine(%)		Oxygen(%)	
	CF_4+H_2	CF_4	CF_4+H_2	CF_4	CF_4+H_2	CF_4
0	33	36	6.5	7	46	34
35	38	…	6	…	39	…
100	52	40	4	6	28	33
135	52	…	4	…	28	…
200	53	48	4.5	8	30	24

The polymer thickness was investigated from Auger depth profile in the previous study [29] and is shown again in Fig. 9. The depth of polymer thickness was a minimum at a magnetic field strength of about 100Gauss. The thickness of polymer layer decreased with the increase of C/F ratio of residue. The residue thickness also decreased with increasing Si etch rate(see Ref. 30 and 31). Therefore, the residue thickness and the C/F ratio of the residue layer and the Si etch rate appear to be related to one another. As the magnetic field strength increases, ion densities bombarding Si surface are increased. Therefore, the residue layer becomes thinner. However, at the same time, as the magnetic field strength increases, the ion bombardment energies decrease. At a certain threshold bias voltage, therefore, the residue can not be sputtered off effectively and the thickness of residue layer starts to increase. The change in Si etch rate and C/F ratio appear to be the result of the change in the thickness of residue layer. For CHF_3 plasma etched sample, similar trends were observed.

The thickness of residue layer estimated from AES was compared with the thickness of residue layer measured with TEM. The thickness of residue layers measured with TEM showed similar results as those measured with AES. The thickness of residue layer estimated from TEM was about 2 to 7nm.

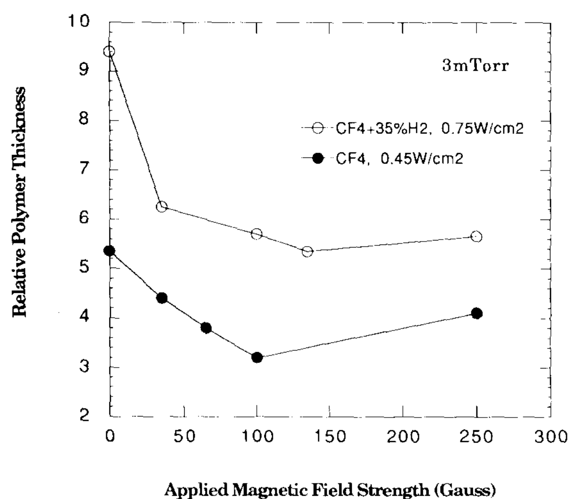

Fig. 9. The thickness of polymer layers estimated from AES depth profiles.

b. Secondary Ion Mass Spectroscopy(SIMS)

For the plasma containing hydrogen, hydrogen ions tend to penetrate into samples by ion implantation and diffusion, causing hydrogen induced defects and contamination.

To study hydrogen contents in CHF_3 and CF_4+H_2 plasma etched samples, SIMS was used to analyze the depth of penetration using Cs^+ ions. The depth profiles for fluorine and hydrogen of the etched samples are shown in the Fig. 10(a) for CF_4+H_2 plasma etched samples and (b) for CHF_3 plasma etched samples as a function of magnetic fild strengths. As shown in the figures the hydrogen contents in the Si increased as the magnetic field strength decreased. Also it appeared that the depth of hydrogen penetration increased with decreasing magnetic field strength. Fluorine depth profiles also showed a similar trend. The penetration depth of fluorine appeared to be close to that of hydrogen. A separate experiment with a reference sample which was not plasma etched showed that during the initial stage of data acquisition, the specimen tended to heat up showing high intensities of hydrogen and fluorine background signals. The intensities of backgrounds decreased as time went on. There fore the backgrounds of hydrogen and fluorine showed similar trends as the signal depth profiles. The background level was different for different species. Therefore, it turned out that it is difficult to compare the pentration depths between the different species because the background levels are different for each species. However, it was possible to compare penetration depths for an element at different magnetic fields.

Aluminum (from the Al_2O_3 electrode) contamination was also investigated using SIMS using O_2^+ ions as primary sputtering ions as shown in Fig. 11 for CHF_3 plasma etched samples. In this case, the reference signal (background) is also shown. The aluminum contamination decreased as the magnetic field strength incerased.

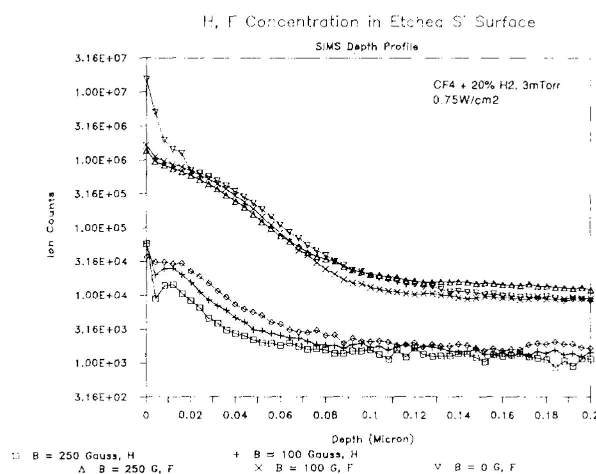

(a)

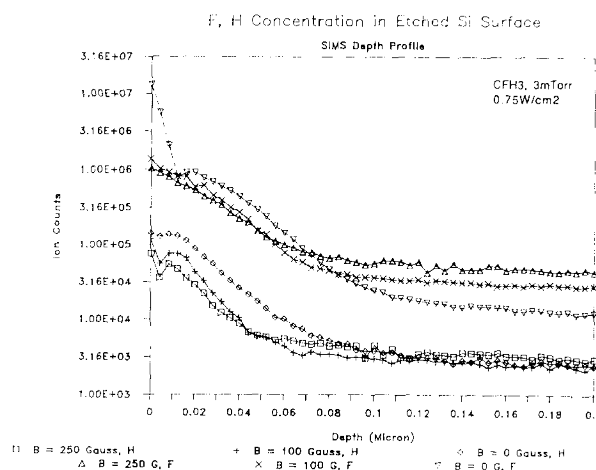

(b)

Fig. 10. a) SIMS depth profiles of fluorine and hydrogen of Si etched with $CF_4+20\%H_2$ plasmas at different magnetic field strengths; b) SIMS depth profiles of fluorine and hydrogen of Si etched with CHF_3 plasmas at different magnetic field strengths.

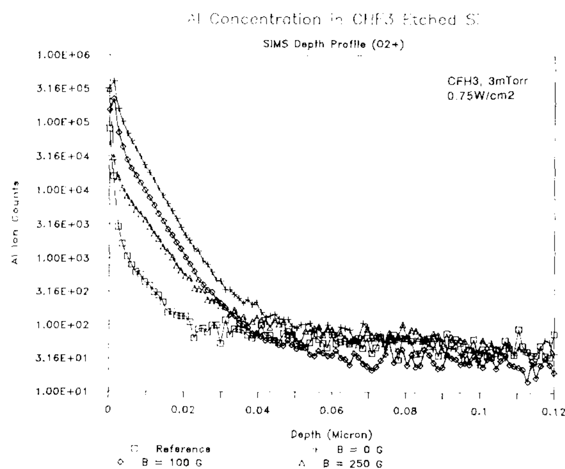

Fig. 11. SIMS depth profiles of aluminum (a target component) of Si etched with CHF_3 plasmas at different magnetic field strengths.

Ⅳ. Discussion

The reduction of radiation damage and contamination of dry etched Si is a goal in sub-micron device fabrication. The reduction of device size also reduces the allowable extent of radiation damage and contamination of the device which must be removed by annealing and cleaning afterwards. In a dc powered magnetron, the addition of magnetic field to the plasma perpendicular to electric field leads electrons to form a circular motion and traps electrons near the cathode[39]. The concept of the magnetron which leads electrons to be trapped near the cathode does not appear to be applicable to rf magnetrons because when the powred electrode has the positive potential during an rf cycle, the trapped electrons are absorbed into the electrode. Even though rf magnetrons do not work with exactly the same functionality as dc magnetrons, the addition of magnetic field to the plasma increases ion and radical densities and reduces ion bombardment energies on the powered electrode.

The advantages of magnetron plasmas have been described as high etch rate and high anisotropy which is obtainable by increasing ion densities, radical densities, and by reduced ion energies as described in previous studies[29~31]. The highest etch rate and most vertical etch profile were obtained by making the bias voltage about 50 V using a combination of certain magnetic field strengths and power densities to the discharge. The advantage of magnetron plasma etching also can be characterized as low damage and contamination to the etched specimen. The Ⅰ-Ⅴ characteristics of Schottky diodes made from etched Si as a function of magnetic field strength show a definite advantage over reactive ion etching by reducing the reverse saturation currents of Schottky diodes. The decrease of reverse saturation current has been observed by Mu et al[15]. for CF_4 RIE samples when Schottky diodes are annealed at the temperature of about 450℃. However, higher reverse saturation currents have observed after annealing for the samples etched with a CF_4+H_2 plasma because annealing removes hydrogen passivation. In case of the magnetron plasma etched samples using CF_4, the reverse saturation currents of the samples etched at magnetic field strengths higher than 100Gauss were close to that of the control sample as shown in Fig. 2. Also, for CF_4+H_2 and CHF_3 plasma etched samples, the leakage currents decreased 2 orders of magnitude at 100Gauss. The increase of leakage currents in Schottky diodes means the degradation of the effective barrier height between metal and semiconductor. The origin of the increase in the saturation current of damaged Schottky diodes has been studied by Singh et al[40]. They demonstrated that it is attributable to the presence of positive charges in the damaged layer, where the positive ions bend the bands downward at the silicon surface.

Structural damage as a function of magnetic field strength showed similar results that are consistent with the Ⅰ-Ⅴ characteristics only if the heavily damaged layers are considered. Deeper heavily damaged layers appeared to form at the lower magnetic field strength condition. The deep defects located on {111} planes shown in the 16, 100 and 250Gauss cases in Figs.5 must be from hydrogen, however, the mechanism of damage is not well understood.

It is interesting to compare the Ⅰ-Ⅴ characteristics with TEM results. The leakage current of CF_4 plasma etched sample at 0Gauss was larger than that of CHF_3 or $CF_4+20\%H_2$ plasma etched samples as shown in Fig. 2. However, the depth of the defects in Fig. 3 was smaller for the CF_4 plasma treated sample. The decrease of leakage current by introducing hydrogen in Si is caused by the passivation of electrical defects by hydrogen even though hydrogen introduces larger physical defects. For the high magnetic field conditions, The leakage currents for CF_4 plasma

etched samples were smaller than that for CHF_3 and CF_4+H_2 plasma etched samples (Fig. 2). Also, the structural defects in the TEM micrographs were smaller for the samples etched with CF_4 plasma. In this case, the damage caused by hydrogen appears to increase electrical defects and cause the leakage current to increase.

The thickness of residue layer did not decrease linearly with increasing magnetic field strength. Instead, it had the minimum thickness in the middle of the magnetic field strength operating range. Also, the highest silicon etch rate was obtained at the minimum residue thickness. This appears to support the theory that the Si etch mechanism is diffusion controlled, as suggested by Oehrlein et al.[10]. Because the etch profile is mostly anisotropic at the highest etch rate condition, if the magnetron is operated near this condition, the thickness of the residue layer can be kept to a minimum.

From the TRIM calculations (Table 1) and SIMS depth profiles (Fig. 10), hydrogen content near the Si surface and hydrogen penetration depth are larger at lower magnetic field conditions. Also, impurities such as cathode material redeposited on the Si are found to the smaller at higher magnetic field conditions, as shown in Fig. 11. Therefore, increasing magnetic field strength tends to reduce undesirable impurity densities in Si.

V. Conculsion

The radiation damage and contamination of magnetron reactive ion etched samples were investigated as a function of magnetic field strength. As the magnetic field strength increased from 0Gauss to 250Gauss, I - V characteristics of Schottky diodes made from reactive ion etched silicon samples improved close to that of the wet etched sample. At 0Gauss, the electrical damage of CF_4 plasma etched samples was higher than that of CF_4+H_2 and CHF_3 plasma etched samples bacause of hydrogen passivation. However, at 100Gauss, the electrical characteristics of CF_4 plasma etched samples were better than that of CF_4+H_2 and CHF_3 plasma etched samples. This could result from the hydrogen induced defects. The thickness of residue layer was minmum at the highest Si etch rate and appeared to be related to the threshold value of ion bombardment energy required to sputter off residue layer and to the densities of ions bombarding the surface. The penetrated hydrogen depth and hydrogen density on the Si surface decreased with increasing magnetic field strength. Also, aluminum, which was sputtered off from the cathode and redeposited on the Si surface, was found to decrease with increasing magnetic field strength. Consequently, the increase of magnetic field strength up to the highest etch rate condition reduced the degree of radiation damage and contamination.

References

1. S. Park, C.P. Sun, J.T. Yeh, J.K. Cataldo, and N. Metropolous, "Plasma Processing," ed. by J.W. Coburn, R.A. Gottscho, and D. W. Hess, MRS Symposia Proceedings **68** (1986), p.65.
2. G.S. Oehrlein, R.M. Tromp, J.C. Tsang, Y. H. Lee, and J. Petrillo, J. Electrochem. Soc. **132**, 1411(1985)
3. G.S. Oehrlein, R.M. Tromp, Y.H. Lee, and E.J. Petrillo, Appl. Phys. Lett. **45**, 420 (1984)
4. D.J. Vitkavage and T.M. Mayer, J. Vac. Sci. Technol **B 4**, 1283(1986)
5. G.S. Oehrlein, J.G. Clabes, and P. Spirito, J. Electrochem. Soc. 1002, May(1986)
6. P.J. Astell-Burt, J.A. Cairns, A.K. Cheetham, and R.M. Hazel, Plasma Chem. Plasma Proc. **6**, 417(1986)
7. G.S. Oehrlein C.M. Ransom, S.N. Chakravari, and Y.H. Lee, Appl. Phys. Lett. **46**, 686 (1985).
8. E.Kay, A. Dilks, and D. Seybold, J. Appl.

P)hys. **51**, 5678(1980).
9. X.C. Mu and S.J. Fonash, J. Electrochem. Soc. **137**, 2853(1988).
10. G.S. Oehrlein, H.L. Williams, J. Appl. Phys. **62**, 662(1987).
11. A.J. Bariya, J.P. Mcvittle, J.M. deLarios, and C.W. Frank, Electrochem. Soc. Extended Abstract **88-1**, 137(1988).
12. S.W. Pang, D.D. Rathman, D.J. Silversmith, R.W. Mountain, and P.D. DeGriff, J. Appl. Phys. **54**,3272(1983).
13. J.M. Heddleson, M.W. Horn, S.J. Fonash, and D.C. Nguyen, J. Vac Sci. Technol. **B 6**, 280(1988).
14. J.S. Wang, S.J. Fonash, and S.Ashok, IEEE Elec. Dev. Lett. EDL-4, 432(1983)
15. X.C. Mu, S.J. Fonash, A. Rohatgi, and J. Rieger, Appl. Phys. Lett. **48**, 1147(1986).
16. S. Ashok and A. Mogro-Campero, IEEE Electron Dev. Lett. EDL-4, 145 (1983)
17. X.C. Mu and S.J. Fonash, G.S. Oehrlein, S. N. Chakravarti, C. Parks, and J. Keller, J. Appl. Phys. **59**, 2958(1986).
18. S. Fonash and A. Rohatgi, "Emerging Semiconductor Technology," ed. by D.C. Gupta and P.H. Langer, ASTM Publication 960, Philadelphia, PA p. 163.(1986)
19. T. Hata, J. Kawahara, and K. Toriyama, Jappan J. Appl. Phys. **22**, 505 (1983).
20. S.W. Pang, M.W. Geis, N.N. Efremow, and G.A. Lincoln, J. Vac. Sci. Technol **B 3**, 398 (1985).
21. H. Cerva, E.G. Mohr, and Oppolzer, J. Vac. Sci. Technol. **B 5**, 590 (1987).
22. S.J. Jeng, G.S. Oehrlein, and G.J. Scilla, Appl. Phys. Lett. **53**, 1735 (1988)
23. J.H. Thomas Ⅲ and L.H. Hammer, J. Vac. Sci. technol. **B 5**, 1617 (1987).
24. S.J. Fonash, R. Singh, A. Rohatgi, P. Rai-Choudhury, P.J. Caplan, and E.H. Poindexter, J.Appl. Phys. **58**, 862 (1985).
25. X.C. Mu, S.J. Fonash, B.Y. Yang, K. Vedam, A. Rohatgi, and J. Rieger, J. Appl. Phys. Ⅲ**58**, 4282 (1985).
26. K. Hirobe and H. Azuma, J. Electrochem. Soc. 939 April (1985).
28. G.S. Oehrlein, A. Bright, and S.W. Robey, J. Vac. Sci. technol. **B 6**, 1650 (1988).
29. G.Y. Yeom and M.J. Kushner, J. Vac. Sci. Technol. **A 7**, 987 (1989)
30. G.Y. Yeom and M.J. Kushner, Appl. Phys. Lett. **56**, 857 (1990)
31. G.Y. Yeom, submitted to Korean J. Mat. Res. (1993)
32. S.J. Fonash, Sol. State Technol., 150 January (1985).
33. A. Rohatgi, M.R. Chin, P. Rai-Choudhury, P. Lester, R. Singh, and S.J. Fonash, a paper presented fall ECS meeting (1983).
34. S.M. Sze, "Semiconductor Devices; Physics and Technology," John Wiley & Sons, New York, p.167 (1985).
35. Trim-89 IBM/PC Software by J. Ziegler, J. Biersack, and G. Cuomo, "The Stopping and Range of Ions in Matter," by J.F. Ziegler, J.P. Biersack, and U. Littmark, Pergamon Press, New York (1989).
36. D.J. Thomson and C.R. Helms, "Plasma Processing," ed. by J.W. Coburn, R.A. Gottscho, and D.W. Hess, MRS Symposia Proceedings **68** p.441 (1986).
37. G. Gildenblat, B.A. Heath, and W. Katz, J. Appl. Phys. **54**, 1855 (1983).
38. I.W. Wu, R.H. Bruce, J.C. Mikkelsen, Jr., R.A. Street, T.Y. Huang, and D. Braun, "Plasma Processing," ed. by J.W. Coburn, R.a. Gottscho, and D.W. Hess, MRS Symposia Proceedings **68** (1986), p.381.
39. J.A. Thornton and A.s. Penfold, Chapter Ⅱ-2 in "Thin Film Processes," ed. by J. Vossen and W. Kern, Academic Press, New York p.75 (1978).
40. R. Singh, S.J. Fonash, S. Ashok, P.J. Caplan, J. Shappiro, M. Hage- Ali, and J. Ponpon, J. Vac. Technol. **A 1**, 334 (1983).